The Raised Midpoint Potential of the [2Fe2S] Cluster of Cytochrome bc_1 Is Mediated by Both the Q_o Site Occupants and the Head Domain Position of the Fe−S Protein Subunit†

Jason W. Cooley,‡ Arthur G. Roberts,§ Michael K. Bowman,§,# David M. Kramer,§ and Fevzi Daldal*,‡

Department of Biology, Institute for Plant Sciences, University of Pennsylvania, Philadelphia, Pennsylvania 19104-6018, Institute of Biological Chemistry, Washington State University, Pullman, Washington 99164-6340, and Macromolecular Structure and Dynamics, Battelle Northwest Laboratory, Richland, Washington 99352-0999

Received October 29, 2003; Revised Manuscript Received December 19, 2003

ABSTRACT: We have previously reported that mutant strains of *Rhodobacter capsulatus* that have alanine insertions (+*n*Ala mutants) in the hinge region of the iron sulfur (Fe−S) containing subunit of the bc_1 complex have increased redox midpoint potentials (E_m) for their [2Fe2S] clusters. The alteration of the E_m in these strains, which contain mutations far from the metal binding site, implied that the local environment of the metal center is indirectly altered by a change in the interaction of this subunit with the hydroquinone oxidizing (Q_o) site [Darrouzet, E., Valkova-Valchanova, M., and Daldal, F. (2002) *J. Biol. Chem. 277*, 3464−3470]. Subsequently, the E_m changes have been proposed to be predominantly due to a stronger or more stabilized hydrogen bonding between the reduced [2Fe2S] cluster and the Q_o site inhabitant ubiquinone (Q) [Shinkarev, V. P., Kolling, D. R. J., Miller, T. J., and Crofts, A. R. (2002) *Biochemistry 41*, 14372−14382]. To further investigate this issue, Fe−S protein-Q interactions were monitored by electron paramagnetic resonance (EPR) spectroscopy and the findings indicated that the wild type and mutant proteins interactions with Q are similar. Moreover, when the Q_{pool} was chemically depleted, the E_m of the [2Fe2S] cluster in mutant bc_1 complexes remained more positive than a similarly treated native enzyme (e.g., the [2Fe2S] E_m of the +2Ala mutant was 55 mV more positive than the wild type). These data suggest that the increased E_m of the [2Fe2S] cluster in the +*n*Ala mutants is in part due to the cluster's interaction with Q, and in part to additional factors that are independent of hydrogen bonding to Q. One such factor, the possibility of a different position of the Fe−S at the Q_o site of the mutant proteins versus the native enzyme, was addressed by determining the orientation of the [2Fe2S] cluster in the membrane using EPR spectroscopy. In the case of the +2Ala mutant, the [2Fe2S] cluster orientation in the absence of inhibitor is different than that seen in the native enzyme. However, the +2Ala mutant cluster shared a similar orientation with the native enzyme when both samples were exposed to either stigmatellin or myxothiazol. In addition, Q_{pool} extracted membranes of +2Ala mutant exhibited fewer overall orientations, with the predominant one being more similar to that observed in the non-Q-depleted membranes of the +2Ala mutant than the Q-depleted membranes of a wild-type strain. Therefore, additional component(s) that are independent of Q_o site inhabitants and that originate from the newly observed orientations of the [2Fe2S] clusters in the +*n*Ala mutants also contribute to the increased midpoint potentials of their [2Fe2S] clusters. While the molecular basis of these components remains to be determined, salient implications of these findings in terms of Q_o site catalysis are discussed.

The ubihydroquinone: cytochrome (cyt) *c* oxidoreductase (cyt bc_1)[1] is an essential component of the mitochondrial and most bacterial respiratory electron transport pathways. A sister complex, the cyt b_6f, is also a part of the photosynthetic electron transport chains of the chloroplasts of higher plants and algae as well as of cyanobacteria (*1*−*3*). In bacteria, the cyt bc_1 is typically comprised of three catalytically active subunits that are the cyt *b*, cyt c_1, and the iron sulfur (Fe−S) protein that contains a high potential [2Fe2S] cluster. During a complete turnover, the enzyme oxidizes two hydroquinone (QH_2) molecules to quinones (Q) at its hydroquinone oxidation (Q_o) site and conveys two electrons to a soluble or membrane-attached cyt *c* on one side of the membrane. The enzyme also recycles the two remaining electrons from two QH_2 oxidations to regenerate a QH_2 at its Q reduction (Q_i) site on the opposite side of the membrane. Coupled to these electron-transfer events, the cyt

† This work was supported by NIH grants GM 38237 to F.D., GM 61904 to M.K.B., and NRSA postdoctoral fellowship GM 65791 to J.W.C.

* To whom correspondence should be addressed. E-mail: fdaldal@sas.upenn.edu. Phone: (215) 898-4394; fax: (215) 898-8780.

‡ University of Pennsylvania.

§ Washington State University.

Battelle Northwest Laboratory.

[1] Abbreviations: electron paramagnetic resonance (EPR), [2Fe2S] cluster containing protein (Fe−S), ubiquinone (Q), cytochrome *b* (cyt *b*), ubihydroquinone (QH_2), ubihydroquinone: cytochrome (cyt) *c* oxidoreductase (cyt bc_1), 5-*n*-undecyl-6-hydroxy-4,7-dioxobenzothiazole (UHDBT), quinone reduction site (Q_i), quinone oxidation site (Q_o), midpoint potential (E_m), mosaic spread factor (m_f).

10.1021/bi035938u CCC: $27.50
Published on Web 02/06/2004

bc_1 also translocates protons across the membrane and contributes to the formation of an electrochemical gradient of protons that is used to produce ATP. Remarkably, the enzyme achieves all of these tasks with a small overall thermodynamic driving force (ΔE_m of about 225 mV) via a unique mechanism of electron transfer that bifurcates the two electrons emanating from a single QH_2 oxidation to two different terminal acceptors located at either side of the membrane (for a review see ref *4* or *5*).

Crystallographic evidence first revealed that the [2Fe2S] cluster containing portion (or the head domain) of the Fe−S protein, which is the initial oxidant of QH_2 at the Q_o site, is located at either the surface of cyt *b*, or near the cyt c_1 subunit, or at an intermediate position between, depending on the inhibitor occupancy of the Q_o site (*6*−*10*). Subsequently, several groups have shown biochemically that a large-scale domain movement (i.e., macro-movement) between these positions is essential for multiple turnovers of the enzyme by demonstrating that mutations interfering with the movement yielded nonactive enzymes (*11*, *12*). While the macro-movement of the head domain from the cyt *b* surface to the vicinity of the cyt c_1 allows for favorable distance-dependent coupling for both the QH_2−$[2Fe2S]^{ox}$ cluster, and the $[2Fe2S]^{red}$ cluster−cyt $c_1{}^{ox}$ electron transfer reactions to proceed at physiologically acceptable rates (*7*, *13*), it may also limit unwanted side reactions. Movement of the Fe−S protein, following reduction of its metal center, away from the Q_o site has also been proposed to trigger bifurcation of the two electrons from the QH_2 oxidation to opposite sides of the membrane (*14*). However, arguing against this proposal is the observation that in mutants unable to perform the macro-movement QH_2 oxidation can still proceed under appropriate conditions (*15*). In essence, the movement of the Fe−S protein coupled to an apparent instability of the semiquinone formed at the Q_o site could allow for the seemingly simultaneous transfer of the second electron to the heme b_L (5). In any event, although the critical bifurcation is readily observed experimentally, the mechanistic details still remain unknown and are the focus of many current studies.

Recently, a set of alanine insertion (+*n*Ala) mutations located in the hinge region of the Fe−S protein of *Rhodobacter capsulatus* have been characterized as having impaired or slowed head domain macro-movements from the Q_o site (*12*, *16*−*18*). Interestingly, these mutant enzymes exhibited raised redox midpoint potentials (E_m) for their [2Fe2S] clusters by as much as 140 mV versus the native cyt bc_1 (*12*, *15*, *18*). Moreover, the raised E_m's were not additive with that induced by the addition of the potent Q_o site class I inhibitor stigmatellin (*14*−*15*, *18*), and they could be lowered to a similar value seen with the native enzyme upon the addition of the Q_o site class II inhibitor myxothiazol (*12*). The photosynthetic revertants of these mutants, a single amino acid substitution in the *ef* loop for the +1Ala strain and the loss of one of the added alanine residues in the +2Ala strain, often pointed to protein−protein interactions with the cyt *b* during the macro-movement of the Fe−S head domain to the c_1 position as the cause of the slowed, or the lack of, enzyme turnover (*15*, *17*, *19*). Thus, the overall spectral, kinetic, and thermodynamic changes observed with these mutant enzymes have led to the possibility that the E_m of the [2Fe2S] cluster of the cyt bc_1 might be dependent upon the Fe−S head domain position at the Q_o site (*18*). Subsequently, Shinkarev et al. (2002) have proposed that changes in the strength or stability of a hydrogen bond between the [2Fe2S] cluster and a Q_o site occupant might be sufficient to explain the E_m changes and the lack of mobility observed with various inhibitors or +*n*Ala mutants (*20*). This proposal also implied that electron-transfer coupled to breaking and reforming of the hydrogen bond with Q may explain how the Fe−S protein movement and substrate−product formation may be initiated (*20*, *21*).

To gain a more detailed understanding of these observations and their implications of a possible link between the E_m variations and Q_o catalysis, we have undertaken studies directed at probing whether the E_m changes observed in the +*n*Ala mutants are solely mediated by the interactions of the [2Fe2S] cluster of the Fe−S protein with the Q_o site occupants. Upon extraction of the Q_{pool}, we found that the E_m exhibited by the [2Fe2S] clusters of the mutant decreased while still remaining significantly higher than a similarly treated native enzyme. Furthermore, continuous wave EPR (CW-EPR) analysis of ordered membranes for orientational dependence of the [2Fe2S] cluster spectra revealed that the predominant orientation of the Fe−S protein head domain in a +*n*Ala mutant ($n = 2$) in the absence of inhibitors was different with respect to that of the native enzyme. Overall, the findings indicate that an altered environment of the [2Fe2S] cluster in the +*n*Ala mutants also contributes to their raised E_m. The implications of these findings are discussed in terms of Q_o site catalysis of the cyt bc_1.

MATERIALS AND METHODS

Bacterial Strains and Growth Conditions. All *R. capsulatus* strains were grown in mineral-peptone-yeast-extract enriched media (MPYE) under semi-aerobic conditions in the dark at 35 °C, as described previously (*12*). The construction and growth phenotypes of the mutants used here are also described in ref *12*.

Preparation and Spectroscopic Analysis of Ordered Membrane Samples. Chromatophore membranes were isolated as described previously (*22*). A method of ordered sample preparation was modified from those outlined in refs *23* and *24*. Briefly, chromatophore membranes (>25 mg/mL total protein) treated as appropriate with 5 mM sodium ascorbate and inhibitors were layered onto Mylar strips cut to fit within a quartz EPR tube (707-SQ-250, Wilmad Glass Inc.). Mylar strips were held in place by glass frames, and dried for 48−72 h under an approximately 80% humidity controlled chamber using saturated $ZnCl_2$. Additional aliquots of chromatophore membranes were deposited on top of the previously dried layers until the desired sample quantity on the Mylar sheet was reached. In this way, cyt bc_1 containing chromatophore membranes were compressed into a very small sample volume, enhancing the signal size two to three times over what can be achieved using frozen liquid chromatophore samples. The signal was further increased by the mutual alignment of the *g*-tensor axis with respect to the magnetic field. Hence, the signal-to-noise ratio for the EPR spectra thus obtained was excellent. Using layered membrane samples, EPR spectra were recorded between 0° to 180° from the magnetic field vector using 5° rotational intervals for 0° to 120° and 10° steps thereafter. Analyses

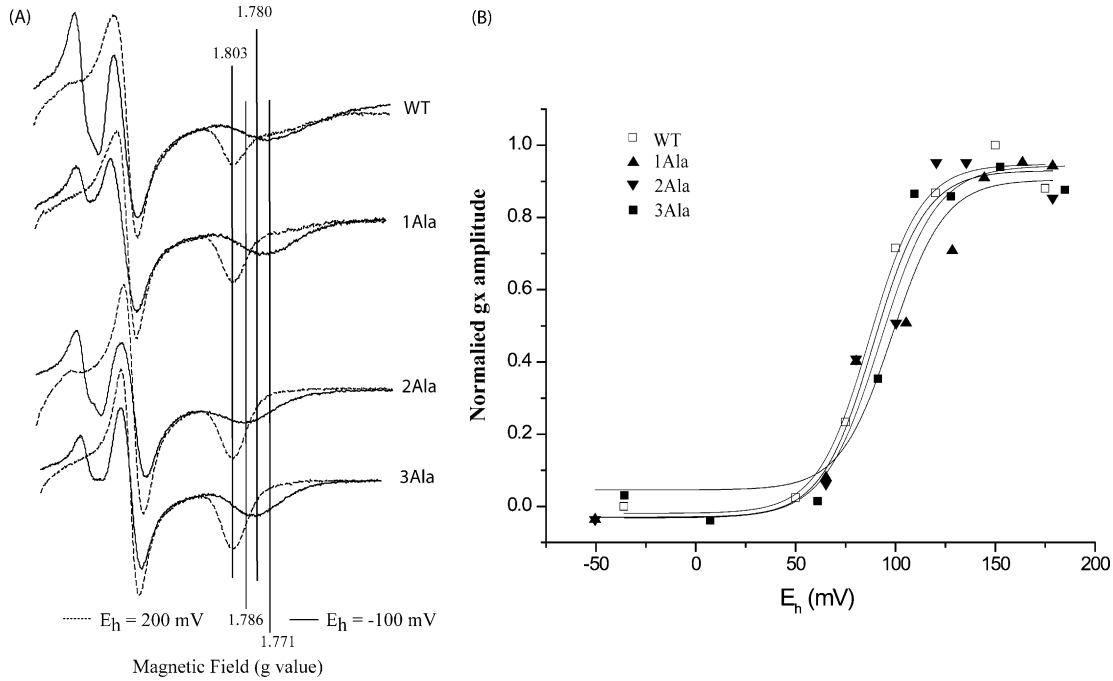

FIGURE 1: Potentiometric dark titrations of the EPR g_x transition of the [2Fe2S] cluster of the Fe−S protein in the wild type and the +*n*Ala mutants. Q_{pool} reduced or Q_{pool} oxidized EPR spectra (A) taken at −100 (solid lines) and +200 (dotted lines) mV, respectively, are shown, and in each case the corresponding g_x transition *g*-value is indicated by a vertical line. EPR spectra were recorded at 20 K, 9.45 GHz with modulation amplitude of 12 G, and microwave power attenuated to 2 mW. Chromatophore membranes isolated from wild type (open squares) and +1Ala (closed up triangles), +2Ala (closed down triangles), and +3Ala (closed squares) mutants were titrated (B) as described in Materials and Methods in the E_h range of −50 and 200 mV. In each case, normalized g_x 1.80 amplitudes (with the minimum amplitude subtracted from each) were fitted to a $n = 2$ Nernst equation.

of the data obtained were carried out as described in ref *23* to deduce the amplitudes of various EPR transitions corresponding to the [2Fe2S] cluster of the cyt bc_1 as follows. (g_z) transition: in the chromatophore membranes, because a cyt bc_1 independent signal overlaps with the g_z region of the [2Fe2S] EPR spectrum only the low field shoulder of this transition was used in quantifying its amplitude; (g_y) transition: the derivative shaped signal of the g_y transition was integrated from baseline to baseline as this proved to be the most consistent means of measurement, free of the effect of any *g*-strain associated with orientation dependence; (g_x) transition: the maximum amplitude of this transition versus a point on the baseline that is orientation neutral (typically, the high field end of the spectrum) was recorded. The g_x signal in many of the samples approaches that of a derivative signal because of the high degree of orientation of the sample. Very little difference was observed between the values derived from the measurements that used peak intensities rather than integration of the peaks. The mathematical simulation of the orientation dependence of the EPR amplitudes was described in detail elsewhere (*23*).

Potentiometric Titrations and EPR Spectroscopy. Potentiometric titrations were carried out as described in ref *25*, except that potassium hexachloroiridate was used in lieu of potassium ferricyanide at redox poises (E_h's) greater than approximately 450 mV, as in ref *17*. EPR spectroscopy was carried out at liquid helium temperatures using a Bruker ESP 300E spectrometer (Bruker Biosciences), fitted with an Oxford instruments ESR-9 helium cryostat (Oxford Instrumentation Inc.). For orientation-dependent spectral acquisition, a goniometer of homemade design, sufficient for consistent reproduction of angular values (±2.5°), was utilized.

RESULTS

The Increase in the E_{m7} of the +2Ala Strain [2Fe2S] Cluster Is Not Due to a Change of the Stability of the Reduced [2Fe2S]−UQH_2 or −UQ Complexes. It is known that class II Q_o site inhibitors such as stigmatellin (*26*) or UHDBT (*27*, *28*) considerably increase the E_m of the [2Fe2S] cluster of the Fe−S subunit of the cyt bc_1 by stabilizing its reduced form, while class I Q_o site inhibitors such as myxothiazol or MOA-stilbene decrease it slightly (*20*, *29*, *30*). Moreover, the EPR g_x transition of the [2Fe2S] cluster of the Fe−S protein responds to the Q_{pool} redox state, with the $g_x = 1.8$ signal titrating with an E_{m7} of approximately 90 mV (*31*). The g_x transition changes from a narrow $g = 1.80$ trough when the Q_{pool} is oxidized to a broader $g = 1.77$ trough when the Q_{pool} is reduced, and to a very broad $g = 1.76$ signal when Q/QH_2 depleted membranes were used. These changes have earlier been interpreted as an indication of the interactions between the [2Fe2S] cluster and the Q/QH_2 molecules residing at the Q_o site (*32*). Thus, to probe any possible link between the increased E_m's observed in mutants affecting the linker region of the Fe−S subunit and the Q_o site residents, we had previously determined the E_m by titrating the amplitude of the $g_x = 1.8$ signal exhibited by the 6Pro mutant, and found that it was unaffected (*18*). Following the proposal of Shinkarev et al. (*20*) that a more stable or stronger interaction between the reduced [2Fe2S] cluster and Q residing at the Q_o site could explain the increased [2Fe2S] cluster E_m's observed in the Fe−S subunit linker domain mutants, we have extended this analysis to the +*n*Ala mutants (Figure 1A). Accordingly, the assumption here being that if the reduced form of the [2Fe2S] cluster is stabilized by a stronger interaction with UQ then the E_m of

the g_x signal transition should become lower (or the oxidized form of the UQ at the Q_o site should be stabilized).

Titration of the amplitude of the $g_x = 1.80$ transition in these mutants as a function of E_h from 0 to 200 mV revealed that in no case did the E_{m7} (approximately 90 mV) change significantly from that observed in the wild type (Figure 1B). These data indicated that neither Q, nor QH_2, formed a more stable complex with the reduced [2Fe2S] cluster of the Fe−S subunit in the mutant strains than the wild type. Interestingly, we noted that at lower E_h's (<50 mV) where the Q_{pool} was predominantly reduced, the line widths of the [2Fe2S] EPR spectra of the +2Ala and +3Ala strains were narrower than that seen with the wild-type strain (Figure 1A). Upon Q_{pool} reduction, the g_x transition shifted from 1.803 to 1.786 or 1.805 to 1.780 in the +2Ala or +3Ala mutants, respectively, while it shifted from 1.803 to 1.771 in the wild-type strains under similar conditions. The larger values of g_x seen with the +2Ala and +3Ala strains upon reduction of the Q_{pool} suggested that in the mutants the [2Fe2S] cluster was experiencing a local environment different from that in the wild-type cyt bc_1. This suggestion led us to probe whether their Fe−S protein head domains were in different positions from that of the native cyt bc_1.

The Orientation of the [2Fe2S] Cluster in the +2Ala cyt bc_1 Relative to the Membrane Plane Is Different from that of the Wild-Type cyt bc_1 Complex. To further probe the altered environment of the [2Fe2S] cluster of the Fe−S subunit in the +2Ala mutant, the angular dependence of the EPR signal of this metal cluster with respect to the membrane plane was monitored using ordered membrane preparations. This technique has been used previously to determine the orientations of the [2Fe2S] clusters of the Fe−S subunits from cyt bc_1 or cyt b_6f treated with different Q_o site inhibitors or metal ions (*23*, *24*, *33*, *34*, *35*). In this case, Mylar-based ordered membrane samples were prepared from the wild type and the +*n*Ala strains in the presence and absence of the Q_o site inhibitor stigmatellin, and changes in the intensities of the g_x, g_y, and g_z transitions were recorded upon the rotation of the samples in the cavity of the EPR spectrometer (Figure 2).

To assess the overall ordering of the membrane preparations from sample to sample, the changes in the amplitude of the EPR transition at $g = 3.4$ (Δb_H) corresponding to heme b_H of cyt bc_1 were compared to the maximal g_y transition at $g = 1.90$ ($Maxg_y$) corresponding to the [2Fe2S] signal of the Fe−S subunit. While some variability in the ordering of the membrane preparations on Mylar sheets was observed, only those preparations with a relatively equivalent $\Delta b_H/Maxg_y$ value were used for analysis. The amplitudes of the g_x, g_y, and g_z transitions for each sample were plotted as a function of the angle of the Mylar sheet from the magnetic field vector, from 0° to 180°, to yield "polar plots". Initially, the angular values corresponding to the maximum amplitudes of the *g* transitions were estimated visually (Figure 3).

Subsequently, more quantitative global simulations of the polar plots derived from the changes in amplitude in the three *g* transitions for each spectrum were carried out as previously reported in ref *23* (see Materials and Methods). These simulations allowed us to deduce the orientations for the *g* transitions (g_{x-sim}, g_{y-sim}, g_{z-sim}) of the predominant population of [2Fe2S] clusters of the Fe−S subunit versus the membrane plane.

Stigmatellin-treated samples yielded similar orientations versus the membrane plane for the [2Fe2S] clusters of the Fe−S subunits in all strains ($g_{x-sim} = 80° \pm 2$, $g_{y-sim} = 0° \pm 5$, $g_{z-sim} = 7° \pm 5$ with a mosaic spread factor (m_f) (a number that describes the relative disorder within a sample (*23*) and can be thought of as a measure of the scatter in orientation of the Fe−S subunit relative to the membrane) of $0.25 \pm 0.05\pi$ rad) (Figure 3A). Thus, all mutants responded to stigmatellin like the wild-type cyt bc_1. Remarkably, simulation of the polar plots corresponding to the +2Ala mutant in the absence of inhibitor required a larger m_f (0.4 versus 0.25π rad for the wild type) to yield the predominant *g*-transition angles (Figure 3B). Simulation of the +2Ala mutant with this m_f value gave g_{x-sim}, g_{y-sim}, and g_{z-sim} that were very different from those of the [2Fe2S] cluster in wild-type cyt bc_1, or in stigmatellin-treated membranes derived from either the wild type or the +2Ala mutant (Figure 3B, gray arrows). The observation of a changed cluster orientation and the high m_f needed for the simulation pointed out that in the uninhibited ascorbate reduced +2Ala mutant cyt bc_1 preparations more than one population of Fe−S subunits with differently oriented [2Fe2S] clusters were present.

Addition of myxothiazol to crystals of bovine cyt bc_1 has been shown to displace the Fe−S head domain away from the *b* position, observed when stigmatellin is in the Q_o site, to another location close to the "intermediate" (*36*) or the c_1 ("distal") (*6*, *36*) positions. In agreement with these crystallographic observations, an increased disorder (or mosaicity) of the [2Fe2S] cluster orientation was observed when myxothiazol was added to membranes derived from either the wild type or +2Ala strains ($m_f = 0.39 \pm 0.05\pi$ rad), as the corresponding polar plots became more ovoid in shape, losing their distinct maxima (Figure 4).

It should be noted that despite the disorder observed with the [2Fe2S] cluster EPR transitions, the overall order of the membranes as judged by the heme b_H EPR transition remained unchanged (data not shown). Therefore, the observed disorder with myxothiazol addition was related solely to disorder in the Fe−S subunits and their orientations. Moreover, when the orientational dependence of the transition amplitudes were simulated, angular values from the membrane plane of $g_{x-sim} = 50°$, $g_{y-sim} = 27°$, and $g_{z-sim} = 27°$ were observed for both the wild type and +2Ala strains. Thus, upon the addition of myxothiazol the Fe−S subunit head domain was allowed a higher degree of rotational freedom in a location away from the "*b* position".

Effects of the Absence of UQ at the Q_o Site on the Thermodynamic Properties and Orientation of the [2Fe2S] Cluster of the cyt bc_1. The presence of an additional [2Fe2S] cluster orientation in the +2Ala cyt bc_1 when no inhibitor is added, and the lack of any appreciable change in the interactions of this metal cluster with Q or QH_2 led us to examine whether the additional orientation reflected a position of the Fe−S subunit head domain independent of Q at the Q_o site, and whether this position contributed to raise the metal center E_m in the +*n*Ala mutants. Isooctane extracted chromatophore membranes that are depleted of the Q_{pool} were prepared, as reported earlier (*29*, *32*) and described briefly in Materials and Methods. Upon complete extraction, membranes derived from +2Ala and wild-type strains

FIGURE 2: EPR spectra of ordered membrane samples showing the [2Fe2S] cluster of the Fe−S protein in the wild type and the +*n*Ala mutants. In each case, maximal g_z and g_y amplitudes (dashed spectra) are observed with the Mylar sheet-membrane plane at 0° from (i.e., parallel to) the magnetic field vector, while the g_x maximum is reached in the spectra recorded when the Mylar sheet-membrane plane is at 90° from (i.e., perpendicular to) the magnetic field vector. Spectra were acquired in the presence (A) or absence (B) of the Q_o site inhibitor stigmatellin (30 μM) with the spectrometer settings the same as those in Figure 1.

contained ≤1.0 Q per reaction center (as estimated by methanol/hexane extraction, data not shown) (*29*, *32*), in agreement with earlier reports (*32*). Complete depletion of the Q_{pool} from the membranes used in these experiments was further confirmed upon their redox titration, as the [2Fe2S] cluster g_x transition seen in the Q-depleted membranes remained unmodified within the E_h range from −100 to 200 mV (Figure 5A).

Interestingly, the g_x transition of the +2Ala mutant Q-depleted membranes CW-EPR powder spectra remained narrower than that seen with similarly treated wild-type membranes (Figure 5A). In addition, Q-depleted membranes from the +2Ala mutant exhibited a [2Fe2S] cluster g_x transition ($g = 1.786$) similar to that seen with non-Q-depleted membranes at poised E_h's where the Q_{pool} was fully reduced (Figure 1B). While the g_x transition of the [2Fe2S] cluster in the Q-depleted +2Ala membranes showed no E_h dependence at low potentials, the amplitude of its g_y transition titrated in the E_h range from 200 to 450 mV revealed an E_m 55 mV more positive than that of similarly treated wild-type membranes (275 mV) (Figure 5B). Therefore, only a fraction of the raised E_m of the +2Ala mutant was due to the interactions between the [2Fe2S] cluster and Q, while the remaining portion appears to be mediated by components other than the Q_o site inhabitants.

To further ascertain the orientation of the [2Fe2S] of the Fe−S subunit in the absence of Q in the Q_o site, ordered membranes were prepared using Q-depleted samples. The layered membranes displayed a level of order similar to those used previously, as assessed by monitoring the $\Delta b_H/\text{Max}g_y$ ratio, indicating that Q depletion did not perturb their ability to be uniformly layered onto Mylar sheets. Remarkably, Q-depleted membrane samples from the +2Ala mutant displayed significantly less mosaic spread as compared to

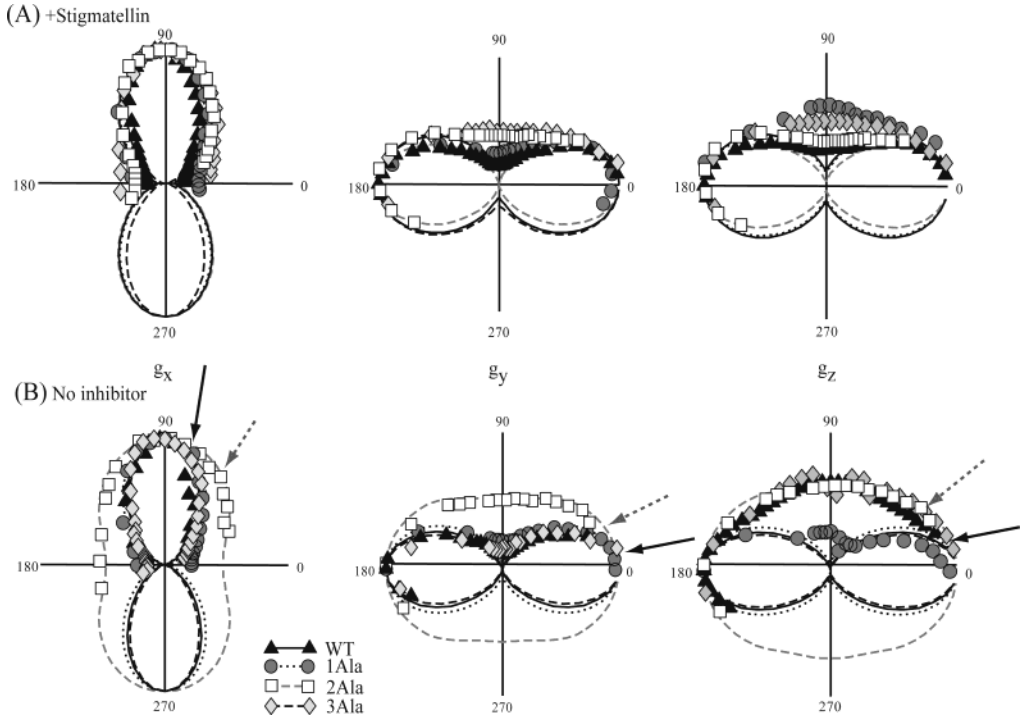

FIGURE 3: Polar plot of the amplitudes of the g_x, g_y, and g_z transitions of the [2Fe2S] cluster of the Fe−S protein in the wild type and +*n*Ala mutants in the presence or absence of stigmatellin. Data obtained with the wild type (closed triangles), +1Ala (closed circles), +2Ala (open squares), and +3Ala (open diamonds) mutants are shown from left to right for the g_x, g_y, and g_z transitions together with calculated fits shown as solid lines. Note that the maximum in the g_x transition amplitudes is near the 90°−270° axis, while the g_y and g_z maximal amplitudes are symmetric around the 0°−180° axis. The fitting procedure is described in Materials and Methods. Dashed and solid arrows indicate the maxima obtained from fits for the +2Ala mutant and for all other cases (which are identical), respectively. In all cases, panels A or B correspond to the data obtained in the presence or absence of stigmatellin (30 μM).

the Q-containing membranes (0.13 versus approximately 0.40π rad) (Figure 6).

The g_{x-sim}, g_{y-sim}, and g_{z-sim} transitions for these samples, 62°, 21°, 8°, respectively, were very similar to those determined for the noninhibited +2Ala membranes (i.e., 59°, 17°, 22°, respectively). These findings implied that the orientation of the [2Fe2S] cluster revealed upon Q-depletion was also present in the non-Q-depleted samples, but was masked by contributions from other positions induced by the interactions of the head domain with Q present in the Q_o site of the cyt bc_1.

DISCUSSION

Additional Components other than Hydrogen Bonding of [2Fe2S] Cluster to the Q_o Site Occupant Influence the E_m of the Fe−S Protein. Shinkarev et al. proposed that hydrogen bonding of the [2Fe2S] cluster of the Fe−S subunit of the cyt bc_1 with the Q_o site occupants dictates the E_m and EPR spectral changes (i.e., g_x transition position and amplitude), observed in the presence of Q_o site inhibitors such as myxothiazol or stigmatellin, or in the +*n*Ala mutants (*20*). This proposal led to the "spring loaded" mechanism that would control the movement of the head domain from the *b* to the c_1 positions upon QH_2 oxidation (*21*). The spring loaded mechanism was fostered by the observation that a hydrogen bond is easily envisioned between a stigmatellin molecule in the Q_o site and the Fe−S head domain in the *b* position in various cyt bc_1 structures (*6*, *10*). In addition, orientation selective ESEEM measurements by Samoilova et al. (*21*) suggested a similar asymmetric nitrogen hyperfine interaction for the [2Fe2S] cluster of the Fe−S when either stigmatellin or Q was present at the Q_o site. This finding pointed out that these two molecules might form a similar hydrogen bond with one of the [2Fe2S] cluster liganding histidine residues (H161 in chicken numbering) of the Fe−S protein of the cyt bc_1. Together with the finding that addition of myxothiazol to cyt bc_1 crystals causes the [2Fe2S] cluster to move away from its stigmatellin bound position on the cyt *b* surface, the spring loaded model suggested that the increases or decreases in the E_m of the [2Fe2S] cluster upon addition of stigmatellin or myxothiazol, respectively, are the result of the presence, absence, or increased strength of a hydrogen bond between the Fe−S protein head domain with the Q_o site inhabitant (*21*). Furthermore, Shinkarev et al. extended their proposal to encompass similar E_m changes that have also been seen with the +*n*Ala hinge region mutants even in the absence of stigmatellin (*17*). On the other hand, it could also be envisioned that a changed flexibility of the hinge region that undergoes coil-to-helix transitions during the macro-movement alters its spring-like properties, thus causing a greater binding constant of the Fe−S to the Q_o site (*4*, *37*). In any event, the lack of a spring to dissociate the Fe−S head domain from the Q_o site would increase the stability or strength of the hydrogen bonding between the reduced Fe−S protein and the Q_o site inhabitants in these strains. Such an increase in the binding strength could then explain the increased E_m and impaired macro-movement observed with the +*n*Ala hinge mutants (*20*).

These attractive suggestions enticed us to examine in detail the E_m of the EPR $g_x = 1.8$ transition of the [2Fe2S] cluster in various Fe−S protein hinge mutants. The position of the g_x transition is known to reflect the [2Fe2S] clusters

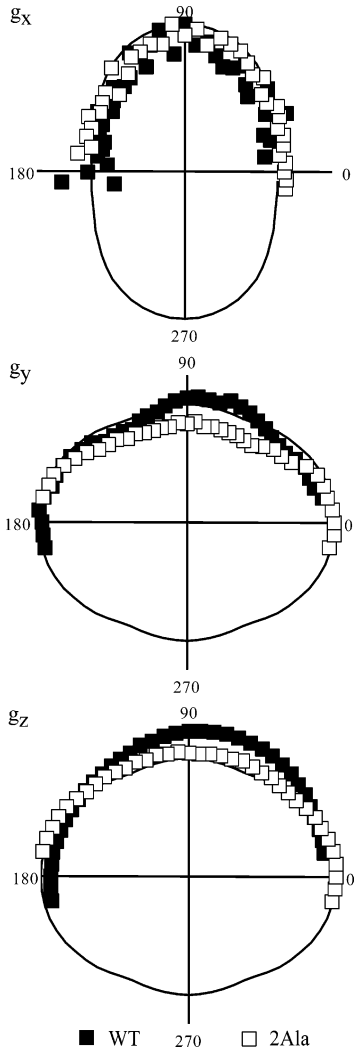

FIGURE 4: Polar plots of the amplitudes of the g_x, g_y, and g_z transitions of the [2Fe2S] cluster of the Fe−S protein in the wild type and +2Ala mutant in the presence of myxothiazol. The wild type (closed squares) and +2Ala (open squares) are shown with solid curves generated from the calculated fits and the spectrometer settings were as in Figure 2.

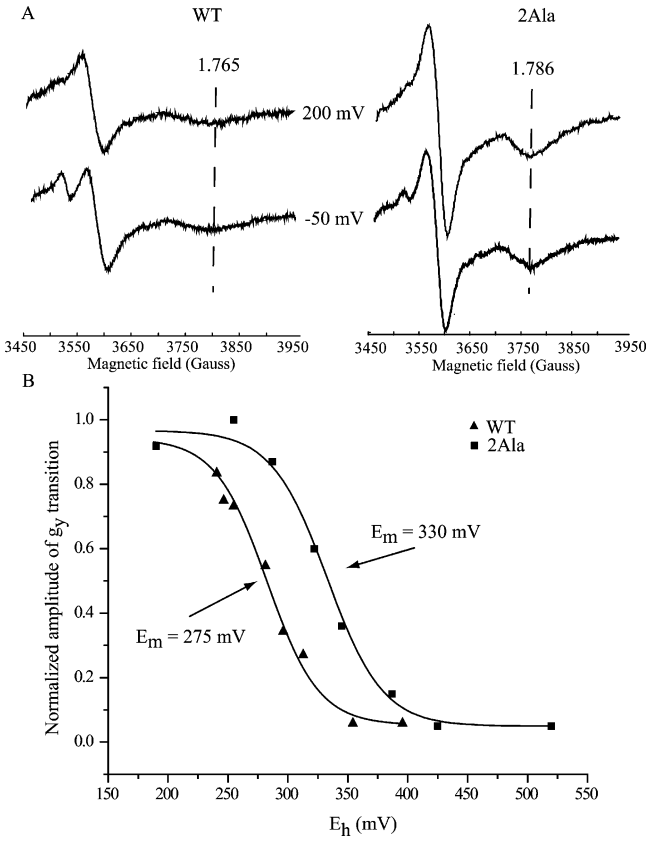

FIGURE 5: EPR spectra and potentiometric dark titrations of the EPR g_x and g_y transitions of the [2Fe2S] cluster of the Fe−S protein in Q-depleted membranes from the wild type and the +2Ala mutants. EPR spectra (A) of isooctane extracted chromatophore membranes prepared as described in Materials and Methods from a wild-type strain (left) and +2Ala mutant (right) of *R. capsulatus* were recorded at E_h's of +200 mV (Q_{pool} oxidized, upper trace) and −50 mV (Q_{pool} reduced, lower trace). Note that the g_x transition at 1.786 observed in Q-depleted membranes from the +2Ala mutant does not respond to the redox potential changes, indicating that no interaction between Q and the reduced [2Fe2S] cluster of the Fe−S protein is detectable. (B) Potentiometric dark titrations of the EPR g_y transition of the [2Fe2S] cluster of the Fe−S protein in Q-depleted membranes of the wild type (triangles) and the +2Ala mutant (squares) between 150 and 550 mV. In each case, normalized g_y amplitudes were fitted to a $n = 1$ Nernst equation to determine the E_{m7}.

interactions with the Q_o site inhabitants (*31*). Thus, any change in the hydrogen-bonding interactions between the $[2Fe2S]^{red}$ and UQ or UQH_2 might also affect the E_m of this EPR transition. Our findings with the +*n*Ala mutants confirm and further extend our previous data from a different kind of hinge mutant (6Pro, where six consecutive residues had been substituted with six prolines), which also has a high E_m for its [2Fe2S] cluster (*12*), in that all showed no significant difference in the E_m's of the EPR $g_x = 1.8$ transitions of the mutants and the wild type (Figure 1). As no difference in the stability of the $[2Fe2S]^{red}$−UQ or $[2Fe2S]^{red}$−UQH_2 complexes could be detected in all cases, the molecular basis of the E_m changes observed in the +*n*Ala mutants cannot be explained solely by the presence, absence, strength, or stability of the His161-UQ hydrogen bond as proposed by ref *20*.

An alternative proposal, originating from the properties of various hinge region mutants and their photosynthesis-proficient revertants, previously suggested that the E_m of the [2Fe2S] cluster of the Fe−S protein reflects its location at the Q_o site, or simply, the interactions of the Fe−S protein head domain with its environment when in various positions (*18*). According to this proposal, the E_m changes seen with various hinge mutations or different Q_o site occupants, including inhibitors, would reflect various populations of the Fe−S head domains in different positions, interacting when possible with both the Q_o site inhabitants as well as other components at the cyt *b* portion of the Q_o site. For instance, different position(s) at the cyt *b* surface may either exclude water from the metal center, or form specific cyt *b* − Fe−S protein−protein interactions as those observed earlier (*19*) or proposed by molecular dynamics simulations of the head domain movement (*38*). Interactions such as these are as likely to perturb the geometry or strength of the hydrogen-bonding network of the [2Fe2S] cluster and affect both the E_m and EPR spectral shape as might a hydrogen bond to the liganding histidine. Similar g_x transitions ($g = 1.786$) are seen in the case of +2Ala mutant when the Q_o site contained either QH_2 or was depleted of Q (Figures 1 and 6). In these cases, we propose that the geometry of the cluster, or of the hydrogen-bonding network around it, are altered producing *g*-values distinctly different from those seen with the soluble

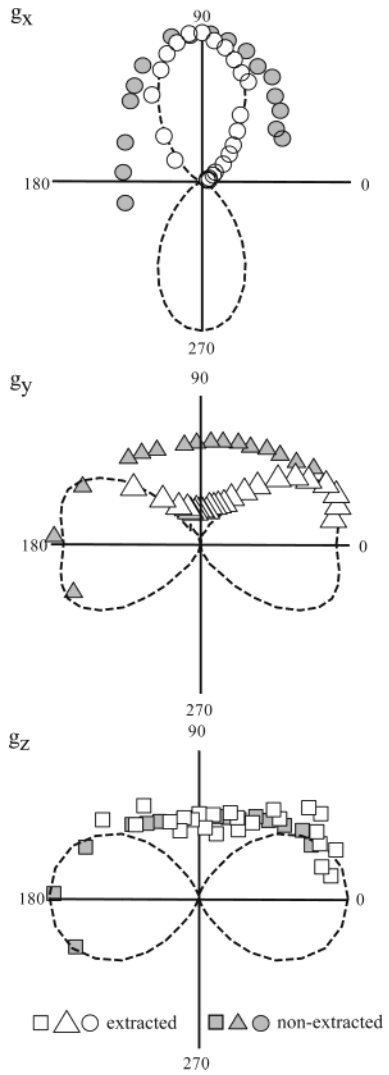

FIGURE 6: Polar plot of the amplitudes of the g_x, g_y, and g_z transitions of the [2Fe2S] cluster of the Fe−S protein in Q-depleted membranes from the +2Ala mutant. Q-depleted (open symbols) and native (shaded symbols) chromatophore membranes were prepared as described in Materials and Methods, and the experimental settings were identical to those described in Figure 3.

($g_x = 1.764$), or myxothiazol ($g_x = 1.77$) treated forms, and even from those that interact with UQ ($g_x = 1.803$) or stigmatellin ($g_x = 1.783$) (*18*). These data are incompatible with the hypothesis that QH_2 or myxothiazol containing cyt bc_1, or the soluble form of the Fe−S subunit, all exhibit similar g_x values attributable to the loss of a hydrogen bond to the [2Fe2S] cluster (*20*). The data presented here with the +*n*Ala strains and previously reported with the 6Pro strain (*18*), clearly indicate that while the EPR spectrum changes in all cases, the extent of broadening and the positions of the EPR transitions are distinct for the different [2Fe2S] clusters when the Q_{pool} is reduced. Overall, our data are more readily accounted for by a change in the position, thus a change in the local environment, of the Fe−S protein head domain at the cyt *b* surface including, but not limited to, the loss or gain of a hydrogen bond via the histidine ligands of its [2Fe-2S] cluster to a Q_o site occupant.

The Orientation in Q-Depleted Membranes Contributes Significantly to Raising the E_m of the [2Fe2S] Cluster of the Fe−S Protein in the +2Ala Mutant. Oriented preparations using Q-depleted membranes of the +2Ala mutant (Figure 5) indicated that the [2Fe2S] cluster of the Fe−S protein in this strain experienced a new environment that is not observed in wild-type membranes lacking Q. The new environment, characterized by a narrower EPR spectrum ($g_x = 1.786$) and a raised E_m of the [2Fe2S] cluster (approximately 330 mV), is independent of the Q_o site inhabitant and its hydrogen-bonding capability. Thus, the EPR line shape and E_m appear to be derived solely from protein−protein or changed solvent interactions resulting from a mutation increasing the length of the Fe−S protein hinge region located over 15 Å away. The E_m of the [2Fe2S] cluster of the +2Ala membranes lacking Q is 55 mV higher than the wild type without Q, while the nonextracted +2Ala bc_1 complex [2Fe2S] cluster has an E_m 90 mV above that of the wild type with Q. Thus, about 50% of the E_m may be attributable in the +2Ala mutant to specific interactions with Q in the Q_o site, while the remainder is the result of differences in the position of the Fe−S head domain.

The exact molecular mechanism of how the cyt *b* environment in this mutant provides this additional stability to the reduced form of the [2Fe2S] cluster is unknown. Along with a perturbation of the strength of a hydrogen-bond interaction of the Q_o site inhabitant to one of the histidine ligands of the [2Fe2S] cluster, a change to a more hydrophobic environment in the presence of Q, an indirect effect of Q binding bringing the head domain to a such a region, or even a combination of all of these factors, could account for the increased E_m of the [2Fe2S] cluster. In particular, any additional hydrogen-bond interaction not originating from the Q_o site occupants would be of particular interest as individual hydrogen-bonding interactions with a high spin iron (Fe^{2+}/Fe^{3+}) can significantly alter the E_m of the metal center (*39*). Obviously, the extended linker region mutants are of relevance for understanding the movements associated with the binding, dissociation, and swinging away of the Fe−S head domain from the cyt *b* Q_o site during QH_2 oxidation in the cyt bc_1.

Multiple Positions of the Fe−S Protein Head Domain. As the Fe−S head domain moves from the *b* surface to a position nearby the c_1 subunit during its macro-movement (*15*), a number of different positions are present simultaneously in the cyt bc_1 population. This heterogeneity makes it difficult to precisely correlate the position of the Fe−S head domain with its chemical properties as, at a first sight, the native enzyme appears to reside in oriented samples in much the same orientation in the presence or absence of stigmatellin (Figure 3A,B). However, it is likely that this orientation is easily detected simply because it is the only fixed position that the wild-type Fe−S head domain can adopt from among the distribution of orientations along its path. The other positions would contribute a relatively broad range of orientations to the overall EPR spectrum and would appear mainly in the orientational spread or m_f. The presence of multiple transient positions is clearly observed in myxothiazol-treated samples, where the fixed position seen in the native enzyme is eliminated by the presence of this inhibitor leaving only the poorly oriented intermediate positions. The g_x transitions seen with myxothiazol or QH_2, albeit broader, are centered at a lower field and have larger amplitudes than that seen with a soluble Fe−S head domain. The limited remaining interactions between the Fe−S protein head domain and the cyt *b* surface could explain why the EPR

spectra obtained in the presence of myxothiazol or at low E_h's are distinct from those obtained with a soluble Fe−S protein head domain fragment.

In view of the problems discussed above regarding the assignment of the EPR g_x transition changes to a single phenomenon, the determination of Q_o site occupancy in different mutant strains must be approached carefully. The mutations themselves, especially those located at the Fe−S protein head domain and cyt *b* interface (*19*, *40*), may cause changes in the position of the Fe−S protein at the Q_o site, independent of the Q_o site occupant. One such case appears to be the +2Ala mutant, as the more rounded shape of the polar plots obtained using ordered membrane preparations, and the need to use a larger m_f to simulate them indicated the presence of multiple subpopulations of the FeS head domain with different orientations. Considering that in the +2Ala mutant the macro-movement of the Fe−S protein head domain is highly restricted (*15*), the range of orientations seen here likely corresponds to various positions that the head domain can explore via small displacements, or micro-movements, at the surface of cyt *b* during Q_o site catalysis (*18*). The fact that one of the observed subpopulations seen with the +2Ala mutant oriented EPR spectra in the absence of inhibitors becomes a homogeneous predominant population in Q-depleted membranes, as implied by a small m_f needed to simulate the predominant *g*-transitions, suggests that at least two major orientationally distinct subpopulations exist in this case. One subpopulation corresponds to Fe−S proteins interacting with Q (with a g_x = 1.8 similar to wild type), and the other one possibly corresponds to a population interacting only with the *b* surface when either QH_2 or no Q (g_x = 1.786) are at the Q_o site (Figure 7). Moreover, in the case of the +2Ala mutant, the EPR spectrum recorded at an angle that yields the maximal g_x amplitude is consistent with multiple components contributing to its shape (e.g., note the broad wing extending to lower *g* values and higher fields from the relatively sharp g_x = 1.80 maxima at approximately 3775 G). An additional transition is discernible in the region of 1.78 (Figure 2), where in the wild type in the absence of inhibitor or in the presence of stigmatellin only a single component is observed.

The orientations of the Fe−S head domain subpopulations seen with the +2Ala mutant either in the absence of inhibitors or in Q-depleted membranes are nearly the same (Figures 3 and 5), which suggests that the orientation might correspond in the native enzyme to a position occupied just after the freshly formed Q molecule leaves the Q_o site and immediately before the arrival of a new QH_2 molecule (Figure 7). This catalytically significant position of the reduced [2Fe2S] cluster is only readily visualized in the +2Ala mutant because the macro-movement of the Fe−S subunit is blocked, presumably by the *ef* loop of the cyt *b* (*17*, *19*). It is more difficult to observe this state in the case of the wild-type cyt bc_1 because the Fe−S subunit would be in many different transient positions with no single dominant orientation (Figure 7). Similarly, when the native membranes are poised at an E_h near 0 mV where the Q_{pool} is completely reduced, the EPR spectrum of the [2Fe2S] cluster reflects those Fe−S head domains that have completed QH_2 oxidation but are not associated with a Q at the Q_o site. As the head domain becomes increasingly hindered in the +2Ala and +3Ala strains, the environments of the [2Fe2S] cluster become more restricted, and hence the EPR line shape is narrower. Thus, this position seen with the +2Ala mutant might be a "resting position" where the only interactions with the Fe−S head domain involve cyt *b* and not Q or QH_2. Such a resting position is reminiscent of the orientations observed in earlier cyt bc_1 structures (*6*, *41*), and with the oriented cyt bc_1 preparations that were frozen with their Fe−S subunits oxidized (*24*).

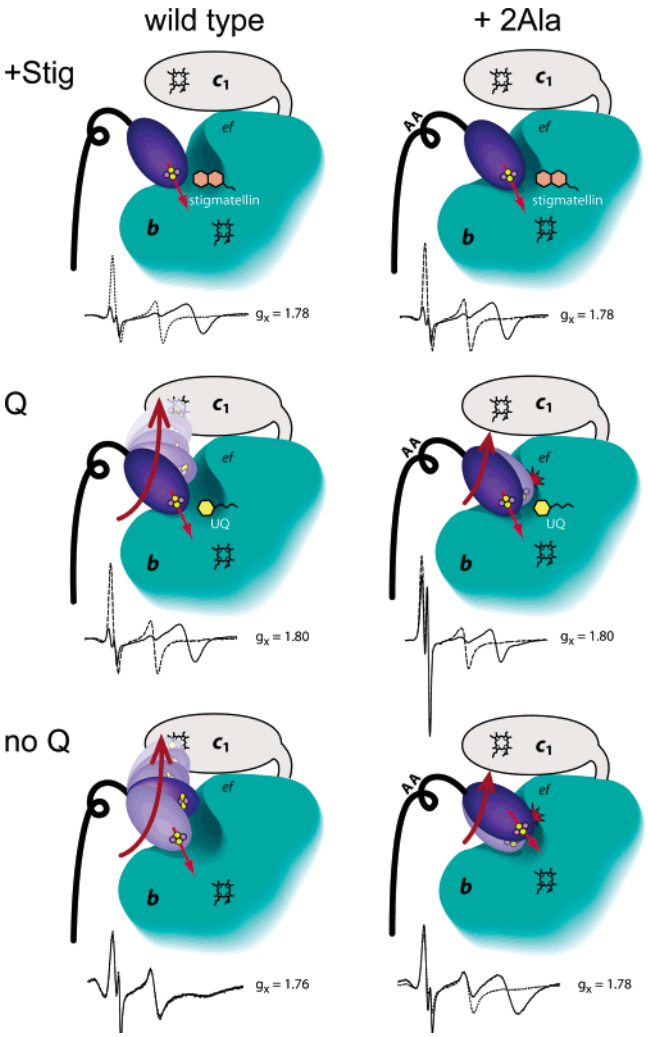

FIGURE 7: Schematic representation of multiple positions of the Fe−S subunit head domain in the presence or absence of Q_o site occupants in wild type and +2Ala mutant cyt bc_1. A portion of the cyt *b* surface (*b*, in blue-green) and its *ef* loop in the vicinity of the Q_o site, drawn as a small cleft for binding of its occupants, and the location of cyt c_1 (c_1, in gray) are depicted. AA refers to the location of the two alanines inserted in the hinge region of the Fe−S subunit. Wild type (left column) and +2Ala (right column) strains with stigmatellin (upper), UQ (middle), no Q (lower) at the Q_o site are shown. Multiple positions of the Fe−S subunit head domain (shades of blue-violet ovals) are shown with a given contribution of each position to the EPR spectrum (shown underneath) indicated by the level of transparency. In both strains, the fixed position of the Fe−S subunit head domain induced by stigmatellin (+Stg) is represented by a single, darkly shaded oval, while its multiple positions in native (Q) and in Q-depleted (no Q) membranes by using multiple shades. In each position, the straight red arrow represents the direction of the Fe−Fe axis of the [2Fe2S] cluster (shown as two yellow and two gray dots), while the curved arrow and its length refers to the span of its mobility, when applicable. In the case of the +2Ala mutant, a red star schematizes the clash of the Fe−S subunit head domain to the *ef* loop of cyt *b*.

In summary, our findings indicate that the position of the head domain of the Fe−S subunit plays a significant role in determining both the shape of the EPR spectrum of the [2Fe2S] cluster and its E_m, both in the presence and in the absence of interactions with Q. Moreover, they reveal that the +*n*Ala hinge mutants that cannot undergo macro-movement can still perform micro-movements of the head domain between the stigmatellin position and the newly found Fe−S head domain position seen in the absence of Q. The significance, if any, of this latter position as a step during Q_o site catalysis, and the precise molecular interactions that affect both the E_m and the EPR *g* factors of the [2Fe2S] cluster remain to be determined in future studies.

ACKNOWLEDGMENT

The authors wish to acknowledge the Johnson Research Foundation for continuous support and maintenance of the EPR facility, without which this work would have been impossible, and Drs. T. Ohnishi and T. Yano for both technical and intellectual advice.

REFERENCES

1. Gennis, R. B., Barquera, B., Hacker, B., van Doren, S. R., Arnaud, S., Crofts, A. R., Davidson, E., Gray, K. A., and Daldal, F. (1993) The bc_1 complexes of *Rhodobacter sphaeroides* and *Rhodobacter capsulatus*. *J. Bioenerg. Biomembr. 25*, 195−209.
2. Darrouzet, E., Valkova-Valchanova, M., Ohnishi, T., and Daldal, F. (1999) Structure and function of the bacterial bc_1 complex: Domain movement, subunit interactions, and emerging rationale engineering attempts. *J. Bioenerg. Biomembr. 31*, 275−288.
3. Cramer, W. A., Soriano, G. M., Ponomarev, M., Huang, D., Zhang, H., Martinez, S. E., and Smith, J. L. (1996) Some new structural aspects and old controversies concerning the cytochrome b_6f complex of oxygenic photosynthesis. *Annu. Rev. Plant Physiol. 47*, 477−508.
4. Berry, E. A., Guergova-Kuras, M., Huang, L. S., and Crofts, A. R. (2000) Structure and function of cytochrome *bc* complexes. *Annu. Rev. Biochem. 69*, 1005−1075.
5. Darrouzet, E., Moser, C. C., Dutton, P. L., and Daldal, F. (2001) Large scale domain movement in cytochrome bc_1: a new device for electron transfer in proteins. *Trends Biol. Sci. 26*, 445−451.
6. Iwata, S., Lee, J. W., Okada, K., Lee, J. K., Iwata, M., Rasmussen, B., Link, T. A., Ramaswamy, S., and Jap, B. K. (1998) Complete structure of the 11-subunit bovine mitochondrial cytochrome bc_1 complex. *Science 281*, 64−71.
7. Kim, H., Xia, D., Yu, C. A., Xia, J. Z., Kachurin, A. M., Zhang, L., Yu, L., and Deisenhofer, J. (1998) Inhibitor binding changes domain mobility in the iron−sulfur protein of the mitochondrial bc_1 complex from bovine heart. *Proc. Natl. Acad. Sci. U.S.A. 95*, 8026−8033.
8. Xia, D., Kim, H., Yu, C. A., Yu, L., Kachurin, A., Zhang, L., and Deisenhofer, J. (1998) A novel electron-transfer mechanism suggested by crystallographic studies of mitochondrial cytochrome bc_1 complex. *Biochem. Cell Biol. 76*, 673−679.
9. Hunte, C., Koepke, J., Lange, C., Rossmanith, T., and Michel, H. (2000) Structure at 2.3 angstrom resolution of the cytochrome bc_1 complex from the yeast *Saccharomyces cerevisiae* cocrystallized with an antibody Fv fragment. *Struct. Folding Des. 8*, 669−684.
10. Zhang, Z. L., Huang, L. S., Shulmeister, V. M., Chi, Y. I., Kim, K. K., Hung, L. W., Crofts, A. R., Berry, E. A., and Kim, S. H. (1998) Electron transfer by domain movement in cytochrome bc_1. *Nature 392*, 677−684.
11. Xiao, K. H., Yu, L., and Yu, C. A. (2000) Confirmation of the involvement of protein domain movement during the catalytic cycle of the cytochrome bc_1 complex by the formation of an intersubunit disulfide bond between cytochrome *b* and the iron−sulfur protein. *J. Biol. Chem. 275*, 38597−38604.
12. Darrouzet, E., Valkova-Valchanova, M., and Daldal, F. (2000) Probing the role of the Fe−S subunit hinge region during Q(o) site catalysis in *Rhodobacter capsulatus* bc_1 complex. *Biochemistry 39*, 15475−15483.
13. Yu, C. A., Xia, D., Kim, H., Deisenhofer, J., Zhang, L., Kachurin, A. M., and Yu, L. (1998) Structural basis of functions of the mitochondrial cytochrome bc_1 complex. *Biochim. Biophys. Acta 1365*, 151−158.
14. Brandt, U. (1999) Control of ubiquinol oxidation at center P (Q_o) of the cytochrome bc_1 complex. *J. Bioenerg. Biomembr. 31*, 243−250.
15. Darrouzet, E., and Daldal, F. (2002) Movement of the iron−sulfur subunit beyond the *ef* loop of cytochrome *b* is required for multiple turnovers of the bc_1 complex but not for single turnover Q_o site catalysis. *J. Biol. Chem. 277*, 3470−3476.
16. Valkova-Valchanova, M., Darrouzet, E., Moomaw, C. R., Slaughter, C. A., and Daldal, F. (2000) Proteolytic cleavage of the Fe−S subunit hinge region of *Rhodobacter capsulatus* bc_1 complex: Effects of inhibitors and mutations. *Biochemistry 39*, 15484−15492.
17. Darrouzet, E., Valkova-Valchanova, M., Moser, C. C., Dutton, P. L., and Daldal, F. (2000) Uncovering the [2Fe2S] domain movement in cytochrome bc_1 and its implications for energy conversion. *Proc. Natl. Acad. Sci. U.S.A. 97*, 4567−4572.
18. Darrouzet, E., Valkova-Valchanova, M., and Daldal, F. (2002) The [2Fe-2S] cluster E_m as an indicator of the iron−sulfur subunit position in the ubihydroquinone oxidation site of the cytochrome bc_1 complex. *J. Biol. Chem. 277*, 3464−3470.
19. Darrouzet, E., and Daldal, F. (2003) Protein−protein interactions between cytochrome *b* and the Fe−S protein subunits during QH_2 oxidation and large-scale domain movement in the bc_1 complex. *Biochemistry 42*, 1499−1507.
20. Shinkarev, V. P., Kolling, D. R. J., Miller, T. J., and Crofts, A. R. (2002) Modulation of the midpoint potential of the [2Fe-2S] Rieske iron sulfur center by Q_o occupants in the bc_1 complex. *Biochemistry 41*, 14372−14382.
21. Samoilova, R. I., Kolling, D., Uzawa, T., Iwasaki, T., Crofts, A. R., and Dikanov, S. A. (2002) The interaction of the Rieske iron−sulfur protein with occupants of the Q_o-site of the bc_1 complex, probed by electron spin−echo envelope modulation. *J. Biol. Chem. 277*, 4605−4608.
22. Atta-Asafo Adjei, E., and Daldal, F. (1991) Size of the amino acid side-chain at position-158 of cytochrome *b* Is critical for an active cytochrome-bc_1 complex and for photosynthetic growth of *Rhodobacter capsulatus*. *Proc. Natl. Acad. Sci. U.S.A. 88*, 492−496.
23. Roberts, A. G., Bowman, M. K., and Kramer, D. M. (2002) Certain metal ions are inhibitors of cytochrome b_6f complex "Rieske" iron−sulfur protein domain movements. *Biochemistry 41*, 4070−4079.
24. Brugna, M., Rodgers, S., Schricker, A., Montoya, G., Kazmeier, M., Nitschke, W., and Sinning, I. (2000) A spectroscopic method for observing the domain movement of the Rieske iron−sulfur protein. *Proc. Natl. Acad. Sci. U.S.A. 97*, 2069−2074.
25. Dutton, P. L. (1978) Redox potentiometry: determination of midpoint potentials of oxidation−reduction components of biological electron-transfer systems. *Methods Enzymol. 54*, 411−435
26. von Jagow, G., and Ohnishi, T. (1985) The Chromone inhibitor stigmatellin binding to the ubiquinol oxidation center at the c-side of the mitochondrial-membrane. *FEBS Lett. 185*, 311−315.
27. Matsuura, K., Bowyer, J. R., Ohnishi, T., and Dutton, P. L. (1983) Inhibition of electron-transfer by 3-alkyl-2-hydroxy-1,4-naphthoquinones in the ubiquinol-cytochrome-c oxidoreductases of *Rhodopseudomonas-sphaeroides* and mammalian mitochondria − Interaction with a ubiquinone-binding site and the Rieske iron−sulfur cluster. *J. Biol. Chem. 258*, 1571−1579.
28. Bowyer, J. R., Dutton, P. L., Prince, R. C., and Crofts, A. R. (1980) The role of the Rieske iron−sulfur center as the electron donor to ferricytochrome c_2 in *Rhodopseudomonas sphaeroides*. *Biochim. Biophys. Acta 592*, 445−460.
29. Sharp, R. E., Gibney, B. R., Palmitessa, A., White, J. L., Dixon, J. A., Moser, C. C., Daldal, F., and Dutton, P. L. (1999) Effect of inhibitors on the ubiquinone binding capacity of the primary energy conversion site in the *Rhodobacter capsulatus* cytochrome bc_1 complex. *Biochemistry 38*, 14973−14980.
30. Crofts, A. R., Barquera, B., Gennis, R. B., Kuras, R., Guergova-Kuras, M., and Berry, E. A. (1999) Mechanism of ubiquinol oxidation by the bc_1 complex: different domains of the quinol binding pocket and their role in the mechanism and binding of inhibitors. *Biochemistry 38*, 15807−15826.

31. Matsuura, K., Packham, N. K., Mueller, P., and Dutton, P. L. (1981) The recognition and redox properties of a component, possibly a quinone, which determines electron-transfer rate in ubiquinone-cytochrome-c oxidoreductase of mitochondria. *FEBS Lett. 131*, 17−22.
32. Ding, H. G., Robertson, D. E., Daldal, F., and Dutton, P. L. (1992) Cytochrome bc_1 complex [2Fe-2S] cluster and its interaction with ubiquinone and ubihydroquinone at the Q_o site − a double-occupancy Q_o site model. *Biochemistry 31*, 3144−3158.
33. Roberts, A. G., and Kramer, D. M. (2001) Inhibitor "double occupancy" in the Q_o pocket of the chloroplast cytochrome b_6f complex. *Biochemistry 40*, 13407−13412.
34. Schoepp, B., Brugna, M., Riedel, A., Nitschke, W., and Kramer, D. M. (1999) The Q_o site inhibitor DBMIB favours the proximal position of the chloroplast Rieske protein and induces a pK-shift of the redox-linked proton. *FEBS Lett. 450*, 245−250.
35. Prince, R. C. (1983) The location, orientation and stiochiometry of the Rieske iron−sulfur cluster in membranes from *Rhodopseudomonas sphaeroides*. *Biochim. Biophys. Acta 723*, 133−138.
36. Iwata, M., Bjorkman, J., and Iwata, S. (1999) Conformational change of the Rieske [2Fe-2S] protein in cytochrome bc_1 complex. *J. Bioenerg. Biomembr. 31*, 169−175.
37. Berry, E. A., and Huang, L.-S. (2003) Observations concerning the quinol oxidation site of the cytochrome bc_1 complex. *FEBS Lett. 555*, 13−20.
38. Israilev, S., Crofts, A. R., Berry, E. A., and Schulten, K. (1999) Steered molecular dynamics simulation of the rieske subunit motion in the cytochrome bc_1 complex. *Biophys J. 77*, 1753−1768.
39. Lin, I. J., Gebel, E. B., Machonkin, T. E., Westler, W. M., and Markley, J. L. (2003) Correlation between hydrogen bond lengths and reduction potentials in *Clostridium pasteurianum* rubredoxin. *J. Am. Chem. Soc. 125*, 1464−1465.
40. Brasseur, G., Sled, V., Liebl, U., Ohnishi, T., and Daldal, F. (1997) The amino-terminal portion of the Rieske iron−sulfur protein contributes to the ubihydroquinone oxidation site catalysis of the *Rhodobacter capsulatus* bc_1 complex. *Biochemistry 36*, 11685−11696.
41. Palsdottir, H., Lojero, C. G, Trumpower, B. L., and Hunte, C. (2003) Structure of the yeast cytochrome bc_1 complex with a hydroxyquinone anion Q_o site inhibitor bound. *J. Biol. Chem. 278*, 31303−31311.

BI035938U